

LA-UR-08- 09-00103

Approved for public release;
distribution is unlimited.

Title: Superconductivity in SrNi₂P₂ Single Crystals

Author(s): F. Ronning, E.D. Bauer, T. Park, J.D. Thompson

Intended for: Phys. Rev. B



Los Alamos National Laboratory, an affirmative action/equal opportunity employer, is operated by the Los Alamos National Security, LLC for the National Nuclear Security Administration of the U.S. Department of Energy under contract DE-AC52-06NA25396. By acceptance of this article, the publisher recognizes that the U.S. Government retains a nonexclusive, royalty-free license to publish or reproduce the published form of this contribution, or to allow others to do so, for U.S. Government purposes. Los Alamos National Laboratory requests that the publisher identify this article as work performed under the auspices of the U.S. Department of Energy. Los Alamos National Laboratory strongly supports academic freedom and a researcher's right to publish; as an institution, however, the Laboratory does not endorse the viewpoint of a publication or guarantee its technical correctness.

Superconductivity in SrNi_2P_2 Single CrystalsF. Ronning¹, E.D. Bauer¹, T. Park^{1,2}, J.D. Thompson¹¹Los Alamos National Laboratory,
Los Alamos, New Mexico 87545, USA²Department of Physics,
Sungkyunkwan University, Suwon 440-746, Korea

(Dated: January 6, 2009)

Heat capacity, magnetic susceptibility, and resistivity of SrNi_2P_2 single crystals are presented, illustrating the structural transition at 325 K, and bulk superconductivity at 1.4 K. The magnitude of T_c , fits to the heat capacity data, the small upper critical field $H_{c2} = 390$ Oe, and $\kappa = 2.1$ suggests a conventional fully gapped superconductor. With applied pressure we find that superconductivity persists into the so-called "collapsed tetragonal" phase, although the transition temperature is monotonically suppressed with increasing pressure. This argues that reduced dimensionality can be a mechanism for increasing the transition temperatures of layered NiP, as well as layered FeAs and NiAs, superconductors.

PACS numbers: 74.10.+v, 74.25.Bt, 74.70.Dd

Introduction:

There has long been attempts to identify structure-property relations which may help to identify the pairing mechanism and how to enhance superconducting transition temperatures. The discovery of superconductivity at 26 K in LaFeAsO^1 has stimulated much work in compounds containing TmPn layers (Tm=transition metal, and Pn = pnictide). The highest transition temperatures to date are found in the ZrCuSiAs structure-type (55 K in $\text{SmFeAs}(\text{O},\text{F})^2$ and 58 K in $(\text{Ca},\text{Nd})\text{FeAsF}$ *there may be a better compound; ref.*), and a correlation has been identified between the As-Fe-As bond angle and T_c ³. Calculations also show that the strength of the magnetic moment sensitively depends on the position of the pnictide relative to the transition metal plane, presumably as this is a way of tuning the hybridization between the pnictide and transition metal (*ref.*). This suggests that structural tuning could have a very dramatic effect on superconducting transition temperatures.

Reasonably large transition temperatures have also been found in the ThCr_2Si_2 structure (ie. 38 K in $(\text{Ba},\text{K})\text{Fe}_2\text{As}_2$)⁴. In the ThCr_2Si_2 structure it has long been known that one can induce an isostructural volume collapse with either substitution or pressure, as one shifts between a bonding and non-bonding state of neighboring Si (or Pnictide) atoms between layers⁵⁻⁹. We will refer to the bonding configuration as the "collapsed tetragonal" structure. Due to the increased bonding between layers, it is natural to anticipate that the collapsed tetragonal phase will be electronically more 3-dimensional than the non-bonding configuration. With FeAs planes the ThCr_2Si_2 structure generally adopts a non-bonding configuration between As atoms from neighboring planes. One exception is that CaFe_2As_2 can be driven into the collapsed tetragonal state with pressure¹⁰. Interestingly, while the homogeneous collapsed tetragonal state does not show signs of superconductivity down to 2 K¹¹, by using different pressure mediums a structurally inhomogeneous scenario is induced¹² which possesses an onset of superconductivity at 13 K^{13,14}. This poses the question of what is the role of the collapsed tetragonal phase (and dimensionality in general) for superconductivity.

We attempt to shed light on this question with a study of SrNi_2P_2 . At ambient pressure SrNi_2P_2 lies in the large tetragonal state above 325 K. Below 325 K the systems possesses an orthorhombic distortion as roughly half of the P atoms adopt a bonding configuration, but the large volume is still preserved. By applying pressure the collapsed tetragonal state can be induced with slight pressure (4 kbar at room temperature)⁶. Here, we identify that SrNi_2P_2 is a bulk superconductor at ambient pressure at 1.4 K. An analysis of the data is consistent with a fully gapped conventional superconductor. By applying pressure we find that the transition temperature is suppressed by less than 50% upon entering the collapsed tetragonal state. Consequently, we conclude that while the collapsed tetragonal state may not be as favorable for supporting superconductivity it is not intrinsically unfavorable to it.

Experimental:

Large, plate-like single crystals of SrNi_2P_2 were grown in Sn flux. The starting materials in the ratio of Sr:Ni:P:Sn=1.3:2:2.3:16 were placed in an alumina crucible and sealed under vacuum in a quartz tube. The contents were then heated to 600 °C for a dwell time of 4 hours followed by 900 °C with a dwell time of 200 hours. Subsequently the charge was cooled to 650 °C at a rate of 3.5 °/hour at which point the excess Sn was spun off with the aid of a centrifuge. Powder X-ray diffraction confirm that the large plate like crystals with typical dimensions 5 x 5 x 0.2 mm³ were SrNi_2P_2 . *Eric, please confirm that this is correct description of the synthesis.*

Specific heat measurements were performed using an adiabatic relaxation technique in a Quantum Design PPMS. Resistance measurements were also performed in a Quantum Design PPMS using a Linear Research resis-

tance bridge with an excitation current of 0.1 mA. Susceptibility measurements were performed in a Quantum Design MPMS with an applied field of 5 T. Results were in good agreement with data at 0.01 T, confirming that no ferromagnetic impurity contribution exists in the sample.

For pressure measurements, a crystal was mounted inside a Teflon cup within a hybrid BeCu/NiCrAl clamp-type pressure cell with silicon oil as the pressure transmitting medium. Because the pressure medium is liquid at room temperature over the pressures used in this study, and that there were no structural transitions below this temperature at the pressures reported, we presume the sample is structurally homogeneous. The cup also contained a small piece of Pb whose known pressure-dependent superconducting transition²⁷ enabled a determination of the pressure within the cell at low temperatures where the superconductivity is measured.

Data:

The in-plane resistivity of SrNi_2P_2 is shown in figure 1, and demonstrates a sharp first order anomaly with thermal hysteresis associated with the structural transition previously observed in X-ray diffraction measurements⁶. Here we find the transition occurs at 325 K upon warming and 320 K upon cooling. The first order transition is further confirmed by magnetic susceptibility measurements shown in figure 2. The susceptibility also shows the first order transition at 325 K (upon warming) and 322 K (upon cooling). *Joe, am I right to think that ZFC is warming, and FC is taken upon cooling?* Interestingly, the susceptibility in the high temperature phase is isotropic, but below the transition becomes anisotropic. While anisotropic g -factors can result in an anisotropic Pauli susceptibility it is surprising that only one structure shows this anisotropy. This suggests that a small magnetic moment may be induced with the structural transition.

The resistivity below the structural transition is characteristic of a good metal with a RRR ($= \rho(300\text{K})/\rho(4\text{K})$) of 40 and a residual resistivity of $1.8 \pm 0.2 \mu\Omega\text{cm}$. At 1.45 K the sample shows a sharp transition in resistivity which is consistent with bulk superconductivity as established by heat capacity measurements shown below. With an applied magnetic field the superconducting transition is rapidly suppressed indicating a very small upper critical field. In addition, with an applied magnetic field there is a slight upturn in the resistivity before the superconducting transition. A similar feature has been observed in other iron based pnictide superconductors and is discussed in ref.²⁸. *Should we mention that the resistivity decreased with the second cool down, but more or less scaled by a geometric factor. To my knowledge we have no explanation for such an effect, and so I prefer not to.*

Specific heat data at low temperatures is shown in figure 3. A fit of the data (not shown) from 1.5 K to 10 K to $C/T = \gamma + \beta T^2 + \delta T^4$ gives $\gamma = 15 \text{ mJ/mol K}^2$ and $\beta = 0.23 \text{ mJ/mol K}^4$ which implies a Debye temperature

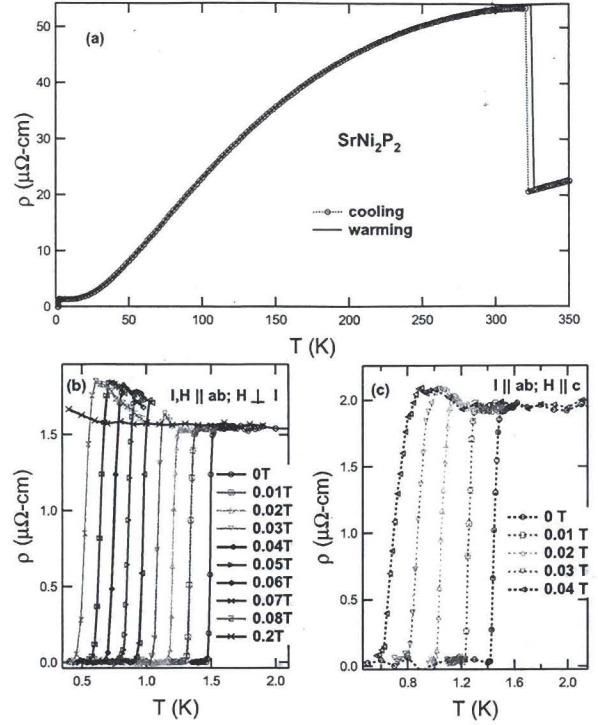


FIG. 1: (color online) In-plane electrical resistivity $\rho(T)$ ($I \parallel ab$) of SrNi_2P_2 (a) for cooling and warming through the structural transition. (b) and (c) show the evolution of the superconducting transition for $H \parallel ab$ and $H \parallel c$, respectively.

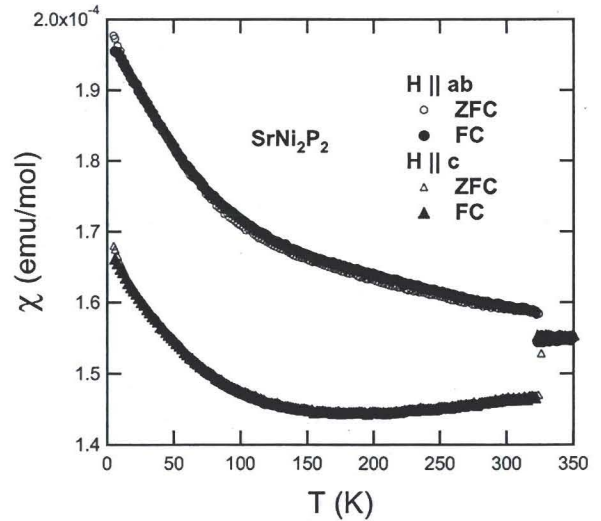


FIG. 2: Susceptibility of SrNi_2P_2 taken as a function of zero-field cooled (ZFC) and field cooled (FC) with an applied field of 5 T.

Θ_D of 348 K. Using a zero temperature susceptibility of $\chi_0 = (2\chi_{ab}(2K) + \chi_c(2K))/3 = 1.86$ emu/mol we find a Wilson Ratio R_W of 0.9 using the expression $R_W = \pi^2 k_B^2 / 3\mu_B^2 (\chi_0 / \gamma)$.

Bulk superconductivity is established by specific heat measurements. By an equal area construction the specific heat gives a transition temperature of 1.415 K, consistent with the drop in resistivity. The fact that the low temperature specific heat gives a jump $\Delta C / \gamma T_c = 1.27$ confirms the bulk nature of superconductivity. From BCS theory we expect the specific heat to be given by the formula

$$C_{\text{BCS}} = t \frac{d}{dt} \int_0^\infty dy \left(-\frac{6\gamma\Delta_0}{k_B\pi^2} \right) [f \ln f + (1-f) \ln(1-f)],$$

where $t = T/T_c$, $f = 1/[\exp(E/k_B T) + 1]$, $E = (\epsilon^2 + \Delta^2)^{1/2}$, $y = \epsilon/\Delta_0$, and $\Delta(T)/\Delta_0$ is taken from the tables of Mühlischlegel²⁹. The specific heat curve obtained by fixing $\gamma = 15$ mJ/molK² from the high temperature fit, $T_c = 1.415$ K and Δ_0 to the weak coupling BCS value $= 1.76 k_B T_c$ is shown by the solid black curve in fig. 3b. Allowing the zero temperature gap value Δ_0 to vary we obtain the dashed blue curve and find $\Delta_0 = 0.201$ meV $= 1.65 k_B T_c$. With the fitted curve to the specific heat, we can extract out the condensation energy and equate it to the thermodynamic critical field giving $H_c = 185$ Oe. The fact that the best fit to the specific heat is *below* the weak coupling value may be caused by pair breaking impurities (*get ref*). We note that in several related superconductors the specific heat jump is also slightly smaller than the weak coupling BCS expectation of $\Delta C / \gamma T_c = 1.43^{23-25,30,31}$.

As mentioned above, the upper critical fields of SrNi_2P_2 are small. In figure 4 the upper critical field deduced from the midpoint of the resistive transition, as well as the midpoint of the specific heat curves are plotted. There is a slight anisotropy observed for the resistivity data. However, the upper critical field as determined by heat capacity is slightly lower as is typically expected, but surprisingly, shows no anisotropy. The slope of the upper critical field from heat capacity is $dH_{c2}/dT_c = -0.039$ T/K. This gives an upper critical field of 390 Oe using the WHH formula $H_{c2}^*(0) = -0.7 T_c dH_{c2}/dT_c$ ³⁴, and a Ginzburg-Landau coherence length $\xi_{GL} = 920$ Å from the expression $H_{c2}(0) = \Phi_0 / 2\pi \xi_{GL}^2$ where $\Phi_0 = 2.07 \cdot 10^{-7}$ Oe cm² is the flux quantum. From the relations $H_c/H_{c1} = H_{c2}/H_c = \sqrt{2}\kappa = \sqrt{2}\lambda_{eff}/\xi_{GL}$ we extract $\kappa = 2.1$, $H_{c1} = 88$ Oe, and $\lambda_{eff} = 1935$ Å.

To investigate the influence of the crystal structure on superconductivity, we applied pressure to SrNi_2P_2 . At room temperature it is known that the orthorhombic structure transforms to a collapsed tetragonal structure at 4 kbar^{6,8}. At lower temperature one would anticipate that this transition occurs at lower pressures. The structural transformation results in a volume change of -3.9% and a -8% change in the c/a ratio⁸. Low temperature resistivity is shown in figure 5a. There is an immediate discontinuous change in the behavior from 0.5 kbar to

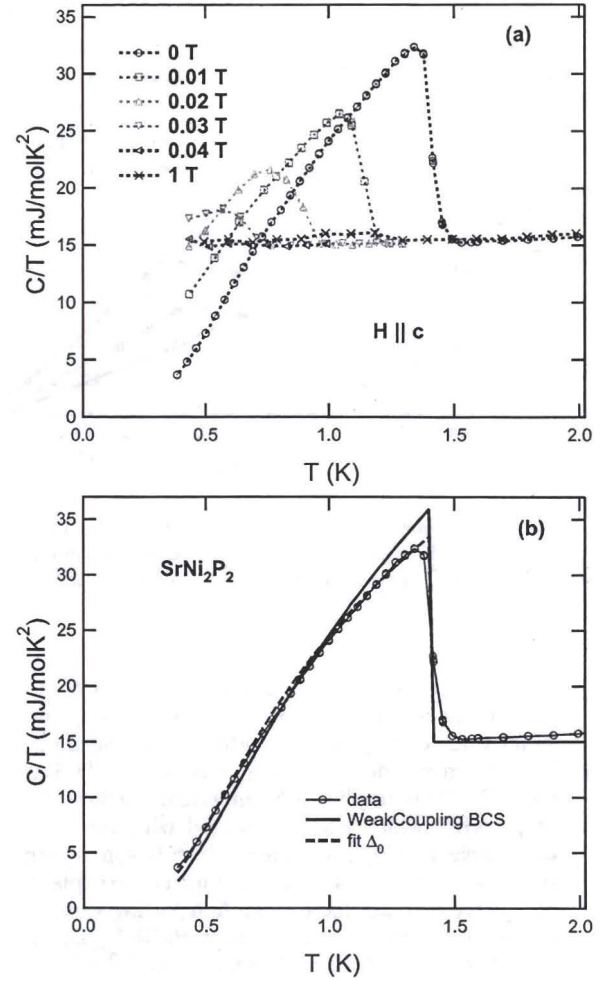


FIG. 3: (color online) (a) Specific heat versus temperature for several magnetic fields applied in the plane of SrNi_2P_2 . (b) The Zero field heat capacity data (circles) along with the theoretical expectation of the specific heat based on a purely weak coupling BCS picture (solid black curve). Fit Δ_0 (dashed blue line) is a fit to the BCS expression holding $T_c = 1.415$ K, $\gamma = 15$ mJ/molK² constant as described in the text.

2.9 kbar. The change in normal state value of the resistivity likely reflects the change in structure which we anticipate with increasing pressure. The superconducting transition temperature decreases monotonically with pressure, although as shown in figure 5b there is a change in slope of T_c versus pressure upon entering the high pressure phase. At 25 kbar there was no superconductivity observed down to 1.8 K. We suggest this is the first transition metal pnictide system which superconducts in the structurally homogeneous collapsed tetragonal phase of the ThCr_2Si_2 structure type.

Discussion:

Several results from the ambient pressure data of

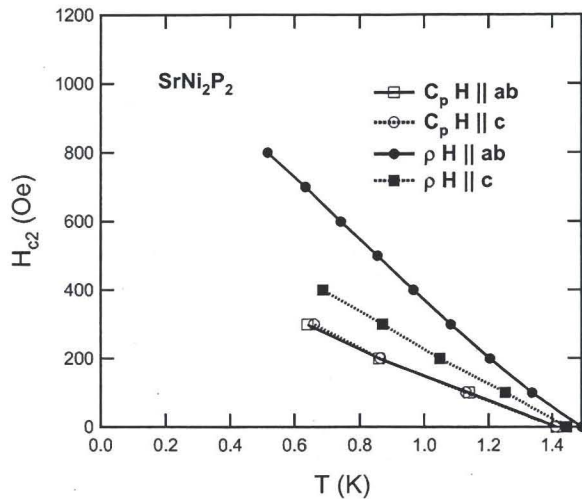


FIG. 4: (color online) Superconducting phase diagram of SrNi_2P_2 as determined by the equal area construction of heat capacity data, and from the midpoint of the resistive transition.

SrNi_2P_2 are suggestive of a fully gapped BCS superconductor, including the fit to the heat capacity data, the small value of H_{c2} and κ . Tight binding calculations for SrNi_2P_2 give a density of states $N(E_F) = 43 \text{ States/Ry Cell}^{9,35}$. This implies a Sommerfeld coefficient of 7.44 mJ/molK^2 , which when compared with the experimentally measured γ , gives an electron-boson renormalization $\lambda = 1.02$. This is certainly sufficient to explain superconductivity in an electron-phonon pairing scenario. Furthermore, calculations show that BaNi_2P_2 has a larger density of states ($\gamma^{th} = 9.32 \text{ mJ/molK}^2$)⁹ which is consistent with its larger superconducting transition temperature ($T_c = 2.7 \text{ K}$)¹⁷. In addition, low temperature thermal conductivity data provide compelling evidence for fully gapped superconductivity in the related material BaNi_2As_2 ³¹. While not a proof, the accumulation of evidence is suggestive that SrNi_2P_2 is a conventional BCS superconductor.

An open question is whether the pairing mechanisms of the Fe based systems and the Ni based compounds are related. On the basis of band structure calculations it has been argued that both $\text{Tm} = \text{Fe}$ and $\text{Tm} = \text{Ni}$ lie close to a magnetic instability *need ref.*; however it remains the case that none of the Ni based systems possess transition temperatures in excess of 5 K ^{15–26} nor do these have evidence for magnetism. Density functional calculations suggest the answer is no, based on the fact that they are unable to reproduce the large transition temperatures of the Fe based compounds^{36,37}. However, it remains a possibility that the pairing mechanisms of the Nickel based systems is merely not as optimized for superconductivity as their iron based cousins.

It is rather remarkable that superconductivity has been found in many of the nickel analogs for which

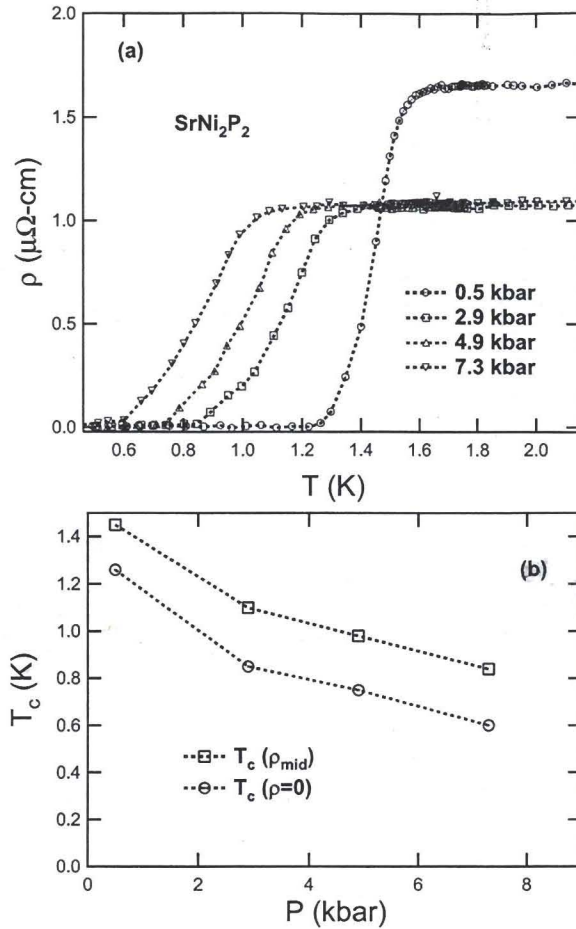


FIG. 5: (color online) (a) Resistivity versus temperature of SrNi_2P_2 for several applied pressures. (b) T_c as a function of pressure as determined by the resistivity in (a) from both the midpoint of the transition (black squares) and the zero resistance state (red circles).

the iron based pnictide also superconducts. Figure 6 shows that even the trend of the maximum superconducting transition temperature decreases monotonically from $\text{ReX}(\text{O},\text{F})$ to BaX_2 to SrX_2 to CaX_2 irrespective of whether $\text{X} = \text{FeAs}$, NiAs , or NiP . A possible interpretation of this trend is that T_c is suppressed with increasing dimensionality. Comparison between the ZrCuSiAs and ThCr_2Si_2 structure types has already established this change in dimensionality³⁸. Within the ThCr_2Si_2 structure this can be further understood from the decreasing ionic radius in going from Ba to Sr to Ca^{5,9}. Consequently, the Pnictide atoms are closer together allowing for stronger hybridization along the z-axis. Eventually this will lead to the collapsed tetragonal state, which should be the most 3-dimensional due to the increased P-P hybridization along the z-direction, and hence the least favorable for superconductivity. Our results, which show

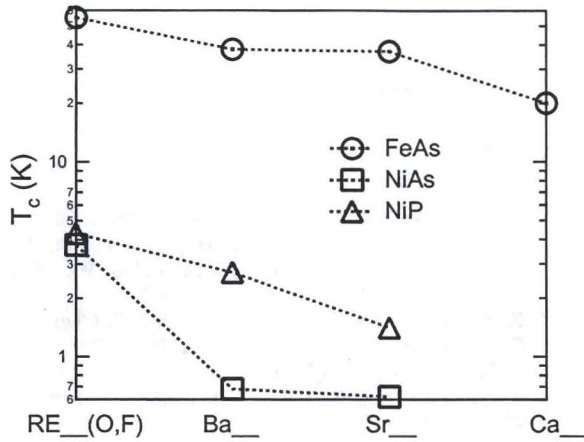


FIG. 6: (color online) (a) Superconducting transition temperature across a few families of compounds for FeAs, NiAs, and NiP planes. For the FeAs series, T_c for SmFeAs(O,F) and for hole doping on the Ba, Sr, Ca site was chosen (refs.^{2, 4, 39, 40}, respectively). T_c for the NiP and NiAs were taken from refs.^{16, 17}, this work and^{19, 23}, and²⁴, respectively.

that superconductivity in SrNi₂P₂ is suppressed upon entering the collapsed tetragonal phase, further support the notion that increased 3-dimensionality found in the collapsed tetragonal state at higher pressures is detrimental

for superconductivity. Further work is needed to determine how precisely dimensionality influences the correlation between families observed in figure 6. Irrespective of the origin of the trend, this work suggests that CaNi₂P₂ and CaNi₂As₂ will be superconducting at temperatures below 1.4 and 0.62 K, respectively.

Conclusion: In conclusion, we have demonstrated that SrNi₂P₂ is a bulk superconductor at ambient pressure at 1.4 K. Upon entering the collapsed tetragonal phase with applied pressure the superconducting transition temperature is monotonically suppressed. Further work is necessary to determine whether SrNi₂P₂ under pressure is the first transition metal-pnictide in the ThCr₂Si₂ structure to possess bulk superconductivity, or whether a similar unknown mechanism as occurs in CaFe₂As₂ is at play. The suppression of T_c with pressure and across families of compounds demonstrates the notion that increased two dimensionality is a mechanism through which higher T_c 's can be achieved.

Acknowledgments

We thank M. Graf for helpful comments. Work at Los Alamos National Laboratory was performed under the auspices of the U.S. Department of Energy.

- ¹ Y. Kamihara, T. Watanabe, M. Hirano, H. Hosono, J. Am. Chem. Soc. **130**, 3296 (2008).
- ² Z.-A. Ren, W. Lu, J. Yang, W. Yi, X.-L. Shen, Z.-C. Li, G.-C. Che, X.-L. Dong, L.-L. Sun, F. Zhou, Z.-X. Zhou, Chin. Phys. Lett. **25**, 2215 (2008).
- ³ C.-H. Lee, T. Ito, A. Iyo, H. Eisaki, H. Kito, M.T. Fernandez-Diaz, K. Kihou, H. Matsuhata, M. Braden, K. Yamada, J. Phys. Soc. Japan **77**, 083704 (2008).
- ⁴ M. Rotter, M. Tegel, D. Johrendt, Phys. Rev. Lett. **101**, 107006 (2008).
- ⁵ R. Hoffmann, C. Zheng, J. Phys. Chem. **89**, 4175 (1985).
- ⁶ V. Keimes, D. Johrendt, A. Mewis, C. Huhnt, W. Schlabit, Z. anorg. allg. Chem. **623**, 1699 (1997).
- ⁷ V. Keimes, A. Hellmann, D. Johrendt, A. Mewis, Th. Woike, Z. anorg. allg. Chem. **624**, 830 (1998).
- ⁸ C. Huhnt, W. Schlabit, A. Wurth, A. Mewis, M. Reehuis, Phys. Rev. B **56**, 13796 (1997).
- ⁹ I.B. Shameem Banu, M. Rajagopalan, M. Yousuf, P. Shenbagaraman, J. Alloys and Compounds **288**, 88 (1999).
- ¹⁰ A. Kreyssig, M.A. Green, Y. Lee, G.D. Samolyuk, P. Zajdel, J.W. Lynn, S.L. Budko, M.S. Torikachvili, N. Ni, S. Nandi, J. Leao, S.J. Poulton, D.N. Argyriou, B.N. Harmon, P.C. Canfield, R.J. McQueeney, A.I. Goldman, Phys. Rev. B **78**, 184517 (2008).
- ¹¹ W. Yu, A.A. Aczel, T.J. Williams, S.L. Budko, N. Ni, P.C. Canfield, G.M. Luke, , arXiv:0811.2554 (2008).
- ¹² A.I. Goldman, et. al., , arXiv:0811.2013 (2008).
- ¹³ T. Park, E. Park, H. Lee, T. Klimczuk, E.D. Bauer, F. Ronning, J.D. Thompson, J. Phys. Cond. Matter **20**, 322204 (2008).
- ¹⁴ M.S. Torikachvili, S.L. Budko, N. Ni, P.C. Canfield, Phys. Rev. Lett. **101**, 057006 (2008).
- ¹⁵ T. Watanabe, H. Yanagi, T. Kamiya, Y. Kamihara, H. Hiramatsu, M. Hirano, H. Hosono, Inorg. Chem. **46**, 7719 (2007).
- ¹⁶ M. Tegel, D. Bichler, D. Johrendt, Solid State Sci. **10**, 193 (2008).
- ¹⁷ T. Mine, H. Yanagi, T. Kamiya, Y. Kamihara, M. Hirano, H. Hosono, Solid State Communications **147**, 111 (2008).
- ¹⁸ T. Watanabe, H. Yanagi, Y. Kamihara, T. Kamiya, M. Hirano, H. Hosono, J. Solid State Chem. **181**, 2117 (2008).
- ¹⁹ L. Fang, H. Yang, P. Cheng, X. Zhu, G. Mu, H.-H. Wen, Phys. Rev. B **78**, 104528 (2008).
- ²⁰ Z. Li, G.F. Chen, J. Dong, G. Li, W.Z. Hu, D. Wu, S.K. Su, P. Zheng, T. Xiang, N.L. Wang, J.L. Luo, Phys. Rev. B **78**, 060504(R) (2008).
- ²¹ J. Ge, S. Cao, J. Zhang, ArXiv:0807.5045 , (2008).
- ²² V.L. Kozhevnikov, O.N. Leonidova, A.L. Ivanovskii, I.R. Shein, B.N. Goshchitskii, A.E. Karkin, ArXiv:0804.4546 , (2008).
- ²³ F. Ronning, N. Kurita, E.D. Bauer, B.L. Scott, T. Park, T. Klimczuk, R. Movshovich, J.D. Thompson, J. Phys.: Cond. Matter **20**, 342203 (2008).
- ²⁴ E.D. Bauer, F. Ronning, B.L. Scott, J.D. Thompson, Phys. Rev. B **78**, 172504 (2008).
- ²⁵ T. Klimczuk, T.M. McQueen, A.J. Williams, Q. Huang, F. Ronning, E.D. Bauer, J.D. Thompson, M.A. Green, R.J. Cava, Phys. Rev. B , in press; ArXiv:0808.1557 (2008).

- ²⁶ H. Fujii, S. Kasahara, J. Phys.: Condens. Matter **20**, 075202 (2008).
- ²⁷ A. Eiling, J.S. Schilling, J. Phys. F **11**, 623 (1981).
- ²⁸ J.G. Analytis, J.-H. Chu, A.S. Erickson, C. Kucharczyk, A. Serafin, A. Carrington, C. Cox, S.M. Kauzlarich, H. Hope, I.R. Fisher, ArXiv , 0810.5368 (2008).
- ²⁹ B. Mühlischlegel, Z. Phys. **155**, 313 (1959).
- ³⁰ S. Kasahara, H. Fujii, H. Takeya, T. Mochiku, A.D. Thakur, K. Hirata, J. Phys.: Condens. Matter **20**, 385204 (2008).
- ³¹ N. Kurita, F. Ronning, Y. Tokiwa, E.D. Bauer, A. Subedi, D.J. Singh, J.D. Thompson, R. Movshovich, ArXiv: , 0811.3426 (2008).
- ³² W. Jeitschko, W.K. Hofmann, L.J. Terbüchte, J. Less Common Met. **137**, 133 (1988).
- ³³ E.H. El Ghadraoui, J.Y. Pivan, R. Guérin, O. Pena, J. Padiou, M. Sergent, Mater. Res. Bull. **23**, 1345 (1988).
- ³⁴ N.R. Werthamer, E. Helfand, P.C. Hohenberg, Phys. Rev. **147**, 295 (1966).
- ³⁵ The calculations of ref.⁹ were performed for an idealized tetragonal form of the structure which neglects the tripling of the size of the unit cell caused by a superstructure of the P position observed in the low temperature structure by⁶.
- ³⁶ A. Subedi, D.J. Singh, and M.H. Du, Phys. Rev. B **78**, 060506 (2008).
- ³⁷ A. Subedi and D.J. Singh, Phys. Rev. B **78**, 132511 (2008).
- ³⁸ ie. M.A. Tanatar, N. Ni, C. Martin, R.T. Gordon, H. Kim, V.G. Kogan, G.D. Samolyuk, S.L. Budko, P.C. Canfield, R. Prozorov, ArXiv:0812.4991 , (2008).
- ³⁹ K. Sasmal, B. Lv, B. Lorenz, A. Guloy, F. Chen, Y. Xue, C.W. Chu, Phys. Rev. Lett. **101**, 107007 (2008).
- ⁴⁰ G. Wu, H. Chen, T. Wu, Y.L. Xie, Y.J. Yan, R.H. Liu, X.F. Wang, J.J. Ying, X.H. Chen, J. Phys.: Condens. Matter **20**, 422201 (2008).